Assessment of Aerosol Optical Depth Measurements from MODIS and AERONET in Thailand, from 2004 to 2023

Piromthong, P. and Satirapod, C.*
Mapping and Positioning from Space (MAPS) Technology Research Center, Department of Survey Engineering, Chulalongkorn University, Thailand
E-mail: pawan.p@chula.ac.th, chalermchon.s@chula.ac.th*
**Corresponding Author*

DOI: https://doi.org/10.52939/ijg.v21i3.4005

Abstract
Air pollution adversely affects human health and the environment. The issue has been raised globally for a long time. Thailand has experienced severe air pollution for decades, particularly in Bangkok, the capital, likely attributable to highly congested traffic, and Chiang Mai, Thailand's second largest city, has been ranked the world's most polluted city several times. To forecast air quality, a sophisticated method like machine learning can be used; however, predefined precision levels and observational parameters must be acquired before being injected into the simulations. This study examines Aerosol Optical Depth (AOD) in Thailand, utilising data from ten AERONET sites and MODIS over a 20-year period, 2004-2023. We evaluate correlations between two observations considering various criteria, including MODIS observational satellites, AOD retrieval algorithms, and the spatiotemporal window sizes utilised in the comparison. The correlations are high in all scenarios (0.72-0.93). Aqua satellite observations have higher correlations than Terra's. The AODs from the Dark Target algorithm exhibit markedly higher correlations than those from the Deep Blue algorithm (0.07-0.17), but the Deep Blue algorithm can retrieve more reliable pixels. Spatiotemporal variation indicates that correlations are more related to observation period duration than spatial window size variations. AERONET measurements indicate seasonal variations in AODs across Thailand, except in the southern region, which exhibits low and stable AOD levels. During the summer, AERONET measurements indicate significantly high AOD levels and considerable daytime variations. This coincides with MODIS observations revealing that northern Thailand has encountered markedly high AOD over a wide area during the summer for the past 20 years. Our investigation revealed that wildfires are probably the primary source of the severe pollution. We analyse time-series AOD across two cities using decompositions. Over the last 20 years, the AOD over Bangkok has increased by ~0.1 while remaining stable over Chiang Mai.

Keywords: AERONET, Aerosol Optical Depth, AOD, MODIS, Thailand

1. Introduction

Air pollution was identified as the second leading cause of death in 2021, resulting in 8.1 million fatalities worldwide [1]. The WHO report states that only approximately 1% of the global population breathes air that meets with WHO standards. Especially, people living in low- and middle-income countries are exposed to ambient PM2.5 concentrations that are 1.3 to 4 times higher than normal. Furthermore, pollution can have a negative effect on the long-term sustainability of the environment as well as the economy, particularly the tourism industry. Thailand has experienced air pollution every year, particularly in the northern part of the country. For many years, Chiang Mai, the largest city in northern Thailand and Thailand's second largest city, has been ranked as the world's most polluted city during summer (February to April). The severe pollution is caused by recurring burning, such as wildfires and agricultural burning. Besides, Bangkok, the capital of Thailand and one of the most congested cities globally, accommodates over 17.4 million residents in its vicinity [2] and hosted more than 20 million visitors in 2023 [3]. It is also affected by pollution, particularly in winter.

For decades, aerosols have been monitored globally by ground-based stations such as the Aerosol Robotic Network (AERONET), and satellite remote sensing platforms, including the Moderate Resolution Imaging Spectroradiometer (MODIS), Ozone Monitoring Instrument (OMI), and Global Ozone Monitoring Experiment (GOME).

Many research projects have conducted these observations across various studies worldwide [4], including in Pakistan and India [5], South Africa [6], the United States ([7][8] and [9]), China ([10] and [11]), Southeast Asia ([12] and [13]) as well as Thailand [14] to characterise aerosols, validate observational accuracies, or utilise them in simulations.

Satellite-based and ground-based observations are essential inputs for simulations or machine learning in air quality modelling and forecasting, which are necessary for managing and mitigating hazards. In the assessment of air pollution with spatial variability, satellite observations offer significant advantages over the ground-based measurements. They provide extensive spatial coverage, able to exceed 100 kilometres per swath, and every pixel in satellite images can provide information, which is highly useful for modelling. They also have the advantage of not requiring maintenance. However, comparing to the remote-sensed measurement taken at approximately 700 kilometres above the Earth's surface, the ground-based measurements can represent aerosol optical depth (AOD) near the surface more precisely than cumulative estimations of the total column in the satellite's line of sight. Also, the ground-based station can provide more useful insights regarding the temporal variability of air quality. Consequently, compensating each other is required. Therefore, validation of satellite-based measurements with ground-based observations is necessary to evaluate the satellite data before it is injected into further simulations.

There are plenty of satellites that provide global air quality monitoring nowadays. In this study, we validate Aerosol Optical Depth (AOD) data obtained from MODIS, which provides long records of observations with high accuracy [15]. This allows for more robust identification of aerosol characteristics. According to the previous study [14], which also examined the correlations between MODIS and ground-based observations from 4 AERONET sites in Thailand, there is still more to be added on. This study analyses 20 years of MODIS AOD data over Thailand from 2004 to 2024 (Figure 1). We compare the MODIS observations to in-situ records of Aeronet AOD from 10 stations in Thailand, which is more than the 4 stations studied by [16], because many stations were only established after 2019. Furthermore, the validation is divided by a variant of MODIS AOD products obtained from Terra and AQUA. According to [9], the AOD retrieved from the Dark Target algorithm exhibits a stronger correlation with ground-based observations in the western United States compared to the Deep Blue algorithm. The performance varies according to the land type. Consequently, we examine Deep Blue and Dark Target products separately in this study. In addition, we vary the temporal and spatial window sizes in our comparisons. This study also displays the availability rates of observations to be expected using a 10x10 km^2 grid across Thailand. We also summarised spatiotemporal variations in AOD from MODIS observations over Thailand, utilising 20 years of data.

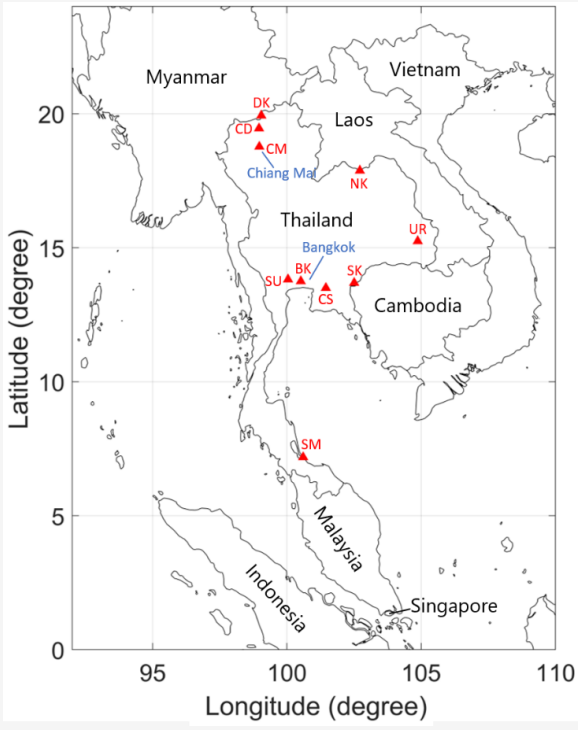

Figure 1: Map of Thailand and its neighbouring countries. The ten AERONET stations in Thailand are depicted with red triangles. Bangkok and Chiang Mai, the largest and second largest cities in Thailand, are pointed by blue lines.

2. Dataset

2.1 MODIS

The Moderate Resolution Imaging Spectroradiometer (MODIS) is a sensor that captures images of the Earth's surface onboard the Aqua and Terra satellites. The sensors provide 36 distinct spectral bands [13], which have been used to enhance comprehension of environmental processes on land, ocean, and atmospheric levels for over 20 years. Specifically, Aqua was launched in 2002, while Terra was launched in 2000. Both satellites are in sun-synchronous near-polar orbits.

Aqua's and Terra's operations can provide global coverage data in 1-2 days. They employ measurements around 1:30 p.m. and 10:30 a.m. local time, respectively. The different acquisition times result in measurements of different AOD conditions that can vary hourly, as described in [17] and Chapter 2.2. Many studies, including [9], demonstrate that the results from Aqua and Terra differ; therefore, we conduct our validations by independently comparing the observations with ground-based measurements.

Furthermore, Aerosol properties products are estimated by Deep Blue (DB) and Dark Target (DT) algorithms, which yield AOD with a spatial resolution of 10x10 km^2 at nadir. The DT algorithm can provide data on both land and ocean, while the DB algorithm can only provide data on land. The two methods have distinct expectations for the Earth's surface and the types of aerosols above it. According to previous research [18], the DT exhibits optimal performance in dark vegetated areas and poorly on bright surfaces. Conversely, the DB is inclusively developed to retrieve AOD over bright surfaces, which are difficult to observe with satellite imagery. As a result, the DB technique is effective in observing AOD in arid and desert areas and it can also provide AOD over highly vegetated areas. For this study, Thailand has natural forests covering 16.6 million hectares (31.47% of total land area) [19] with no desert area. Consequently, both the DB and DT products are expected to provide vulnerable information.

This study employs Level2 MODIS Collection 6.1 aerosol products acquired from 2004 to 2023. The Aqua (MYD04_L2) and Terra (MOD04_L2) products are obtained from the Level-1 and Atmosphere Archive & Distribution System Distributed Active Archive Centre (LAADS DAAC) (https://ladsweb.modaps.eosdis.nasa.gov/). Thailand has been chosen as the area of interest for product searches. In this study, we utilise the values labelled "Deep_Blue_Aerosol_Optical_Depth _550_Land" as Deep Blue AOD and "Optical_Depth_Land_ And_Ocean" as Dark Target AOD. All available pixels with any quality assurance are employed.

2.2 AERONET

The AErosol RObotic NETwork or called AERONET has proven high accuracy for monitoring AOD with an uncertainty of ± (0.01-0.02) [20] and has been utilised in many researches to investigate AOD across the globe over the past two decades. The network is a federated ground-based system for monitoring aerosol optical properties and is primarily managed by NASA Goddard Space Flight Centre [21]. The instruments are spread across the globe and their records of observations are accessible free of charge. Currently, there are 10 AERONET sites located across Thailand (Figure 1 and Table 1), which can be downloaded freely (https://aeronet.gsfc.nasa.gov/new_web/download_all_v3_aod.html). They are used to validate the AOD observed from MODIS in this study. Half of them have been operational for approximately 3-4 years, while the others can provide longer periods of data record.

The monitoring employs sunphotometers [22] and provides measurements at 340, 380, 440, 500, 675, 870, and 1020 nm of spectral bands with high temporal resolution, which can be reached every 15 minutes. The recent processing algorithm, Version 3.0, offers three levels of products based on quality: Level 1.0 (unscreened), Level 1.5 (cloud-screened and quality controlled), and Level 2.0 (quality assured).

Table1: Description of AERONET sites in Thailand

Site no.	Site Name	Acronym	Coordinates		Elevation (m)	Level 1.5		Level 2.0	
			Lon	Lat		Start	End	Start	End
1	Bangkok	BK	100.518	13.749	57	28/1/2019	27/8/2024	28/1/2019	28/6/2023
2	Chachoengsao	CS	101.450	13.500	60	1/2/2021	12/7/2024	1/2/2021	2/6/2023
3	Chiang_Dao	CD	98.961	19.455	450	4/3/2020	19/9/2024	4/3/2020	7/10/2023
4	Chiang_Mai_Met_Sta	CM	98.972	18.771	312	23/9/2006	19/9/2024	2/12/2007	13/10/2023
5	Doi_Ang_Khang	DK	99.045	19.932	1,536	5/2/2013	19/9/2024	5/2/2013	16/12/2023
6	Nong_Khai	NK	102.717	17.877	175	21/1/2015	19/9/2024	21/1/2015	30/6/2023
7	Silpakorn_Univ	SU	100.041	13.819	72	15/8/2006	5/9/2024	30/10/2007	22/12/2023
8	Songkhla_Met_Sta	SM	100.605	7.184	15	11/1/2007	12/9/2024	8/3/2008	9/12/2023
9	Sra_Kaeo	SK	102.504	13.689	68	18/2/2019	14/8/2024	18/2/2019	27/6/2023
10	Ubon_Ratchathani	UR	104.871	15.246	120	2/10/2009	20/9/2024	2/10/2009	17/2/2024

Even though the number of available Level 2.0 data points is slightly lower than Level 1.5, we conduct Level 2.0 product in this study to verify satellite- and ground-based correlations more accurately. As the satellite-based MODIS provide AOD observations at 550 nm, which are not available in AERONET observations, we interpolate AERONET AODs using observations at wavelengths 500 and 675 nm spectral bands, and Angstrom exponents at 440-675 nm (α) by Equation1., as used in [9][23] and [24] to determine the AERONET AOD at 550 nm. λ represents wavelength.

$$AOD_{550nm} = \frac{AOD_{500nm}}{exp\left(-\alpha \times ln\left(\frac{\lambda_{500nm}}{\lambda_{550nm}}\right)\right)}$$

Equation 1

In addition, to gain a better understanding of the overall characteristics of AOD near the surface in Thailand, we present the AOD observations from AERONET in Figure 2. In Figure 2(a), all measurements recorded by the Chiang Mai Met Sta site over the past 16 years are plotted by time of year. We estimate mean AODs every half-month (~15 days) and display them with a blue dotted line. We also show the mean AODs of all ten Thai stations located in Thailand in Figure 2(b). The mean AODs show that nine out of ten stations have significant seasonal variations. The monitoring displays significantly high levels of AODs in summer (February-April), particularly at sites in northern Thailand, CD, CM, and NK, which are probably impacted by wildfires that occur repeatedly during the summer. The Doi Ang Khang site appears to be less affected than the others. This could be due to the station's location on a mountain, 1,536 metres above ground. AOD levels decrease during the transition from summer to fall (April-May).

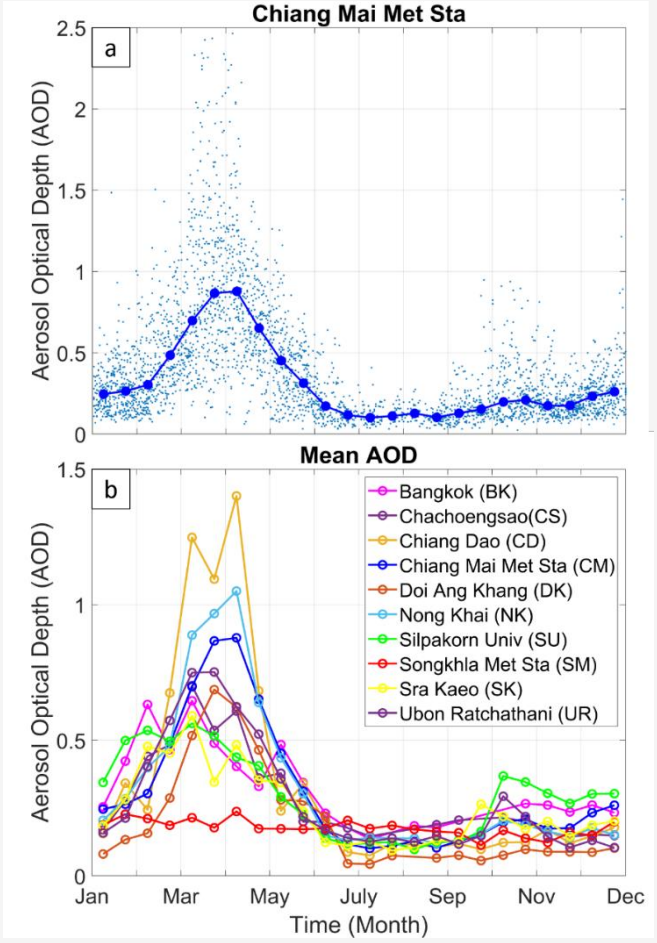

Figure 2: (a) AOD Measurements from the Chiang Mai Met Sta (CM), an AERONET station, recorded from 2007 to the present, represented by blue dots, are shown with month of year. The thick blue-dotted line displays the median values for each half-month. (b) Mean AOD observations from each station in Thailand. They are all plotted against the month of the year and differentiated by colour.

During Thailand's rainy season, from May to October, especially between August and October when there is a lot of rain, AOD levels at all monitoring stations are steadily low, probably attributable to the washing out of rain and wind that comes with rain. These two factors can help to mitigate aerosol mechanisms. During the winter, AOD levels also appear to be stable but slightly higher on average than during the rainy season. Conversely, the Songkhla Met Sta site in southern Thailand is the only site that exhibit low and stable levels of AODs throughout the year. This agrees with the fact that Thailand's southern region is a coastal area with little traffic congestion and few industrial activities.

Furthermore, as the AERONET provides observations with a high temporal resolution which can reach about every 15 minutes during the day, this allows us to investigate the AOD variation hourly throughout the day, which is limited with daily MODIS measurements. Therefore, we present aerosol daytime variations in Figure 3. We calculate the mean AOD every 15 minutes during the daytime using long records of data. Due to the seasonal variations mentioned in the previous paragraph, we divide the data into four periods for analysis. In addition to the significantly higher levels of AOD during the summer, the AERONET observations present significant variations in AOD during the daytime, which differs from the other seasons, which are mostly low and stable throughout the day.

Although the levels of variations vary by stations, the observations from most of stations show similar pattern that AOD levels increase in the early morning, peak in the late morning (around 9 a.m.), and then gradually decrease throughout the day.

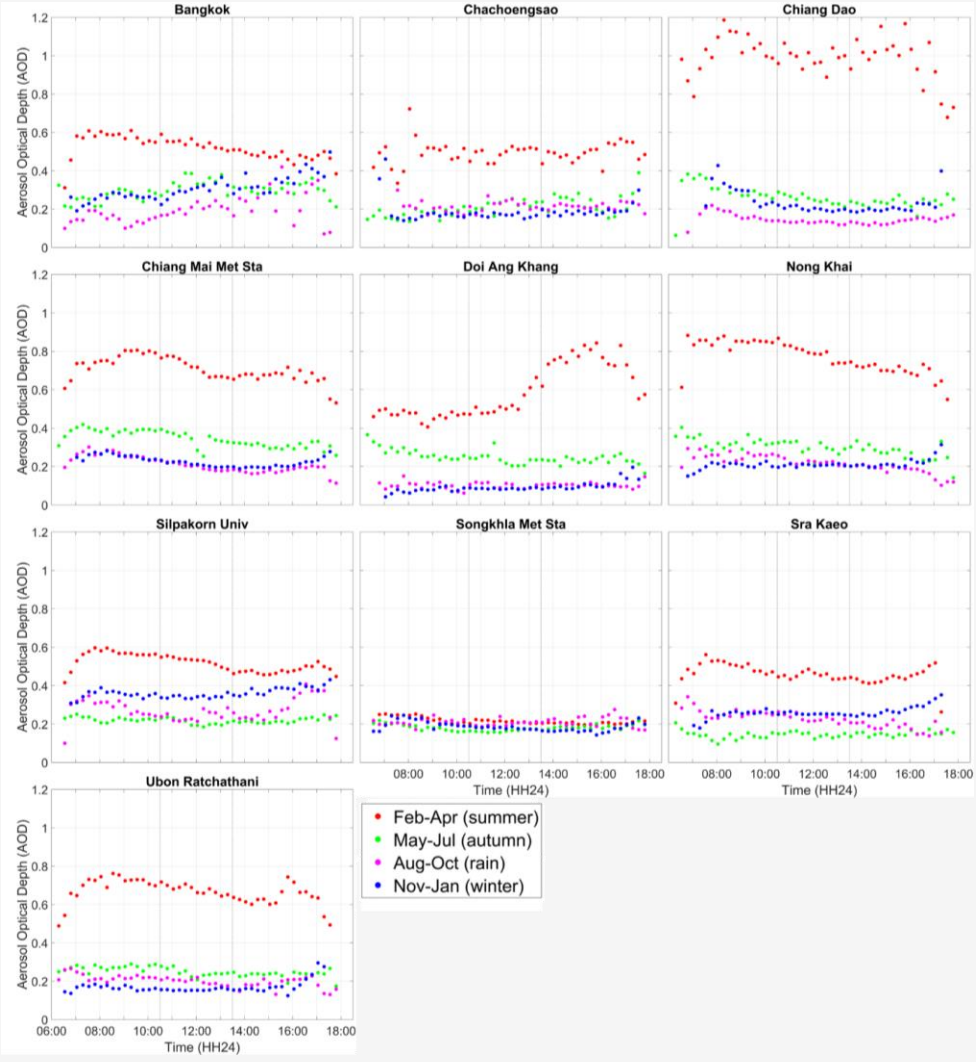

Figure 3: Mean AOD levels at different times of day. The dots are presented every 15 minutes. All calculations are conducted separately for each season. The vertical black lines indicate Terra and Aqua's acquisition times around 10:30 a.m. and 1:30 p.m. local time, respectively.

As previously noted, most of the sites in northern Thailand are impacted by wildfires during the summer; however, the AOD patterns detected from the Chiang Dao and Doi Ang Khang sties appear to differ from the others. The AOD variations observed at the Chiang Dao site may be influenced by wildfires as well as local factors such as location, topography, and human activities, resulting in a significantly different pattern of variation. Conversely, observations from the Doi Ang Khang sites show an increasing trend in the afternoon, with AOD levels remaining high throughout the afternoon before decreasing after 5 p.m. The increase during the day is probably related to mountain flows that transport AOD from the ground to higher elevations, as also found in the western United States [25]. Apart from the summer, AOD levels appear to be less significant from May to July (green dots), but they are higher than in the other two seasons (August-October and November-January). This could be due to that the AOD is still decreasing in May but does not reach the bottom yet; however, they appear to be stable during the daytime. On the other hand, the AOD pattern observed at the Songkhla Met Sta site in the south is clearly different from the other stations, which appear to have no significant pattern.

From the results, we do not allow to conclude whether the AOD levels at ground during the MODIS observations (10:30 a.m. and 1:30 p.m. local time) represent low or high periods of the day. Due to the spatial variability of AOD patterns, when using MODIS satellite data, we need to consider that the AOD levels presented by MODIS do not represent daily AOD.

3. Correlation

This chapter presents correlations between AOD observations from MODIS and ten AERONET stations in Thailand. According to [9], variations in MODIS products and parameters employed in comparisons led to varying correlations in the western United States. Due to the differing weather and topography between Thailand and the United States, we also conduct our validation analysis with feature variance to examine correlation variations in Thailand. We summarise the variances utilised in the comparisons in Table 2. As the performance of AOD retrieval algorithms DB and DT varies depending on land cover, we compare AOD retrieved from each algorithm separately to define a better product for monitoring Thailand AOD. According to satellite trajectories, Aqua and Terra MODIS measure atmospheric AOD at different times of day, approximately 1:30 p.m. and 10:30 a.m. local time, respectively. Therefore, they perceive varying AOD conditions influenced by factors such as temperature, humidity, or human activities. We aim to determine whether the variation in correlations under different circumstances, influenced by the timing of acquisitions throughout the day, is random or exhibits a discernible trend regarding optimal times for acquisition.

Furthermore, we vary the distances of spatial windows when selecting observations from satellite MODIS images. MODIS AOD observations within 10, 20, 30, 40, and 50 kilometres from the AERONET sites are selected for averaging in the comparisons. We also employ varying lengths of temporal windows when selecting measurements from AERONET data for averaging. We compute averages from AERONET AOD measurements taken around the acquisition times (10:30 a.m. for Terra and 1:30 p.m. for Aqua) using window sizes of ±5, ±15, ±30, ±60, ±90 and ±120 minutes, which correspond to 10, 30 minutes, 1, 2, 3, 4 hours, respectively. In addition, we compare daily AOD data product which are already calculated and provided officially online. (https://aeronet.gsfc.nasa.gov/new_web/download_all_v3_aod.html).

This variation can provide some useful information. For example, the spatial variation can specify the number of pixels required in filtering to achieve optimistic results. Because of the poor temporal resolution of satellite-based observations, once every 1-2 days for MODIS, the temporal variation can define periods of time during which MODIS observations can represent AOD levels with acceptable correlations to ground-based measurements. Furthermore, due to the frequent absences of reliable satellite-based measurement in tropical region, such as Thailand, where clouds cover almost the entire year, this study can illustrate how large the spatial and temporal windows can be expanded to include a greater number of samples with a desired level of correlation.

All of the variations discussed above are used to compare available pairs of observations when that both MODIS (2004-2023) and AERONET (Table 1) observations are available.

Table 2: Variance parameters utilised in comparisons

Par No.	Parameter	Variation
1	Satellites	Terra, Aqua
2	Algorithm	Deep Blue (DB), Dark Target (DT)
3	Temporal window	±10, ±15, ±30, ±60, ±90, ±120 mins and daily
4	Spatial window	10, 20, 30, 40, and 50 km

According to [9], the variations in correlations, caused by different spatiotemporal window sizes vary by stations and appear random. Specifically, for example, increasing the temporal window size causes correlations to increase at some stations while decreasing at others, with no apparent spatial pattern. Therefore, we perform our analysis using all observations from every station in Thailand to define averaged correlations rather than defining them individually. We show scatter plots of AERONET measurements and MODIS observations (Terra DB, Terra DT, Aqua DB, and Aqua DT) in Figures 4-7.

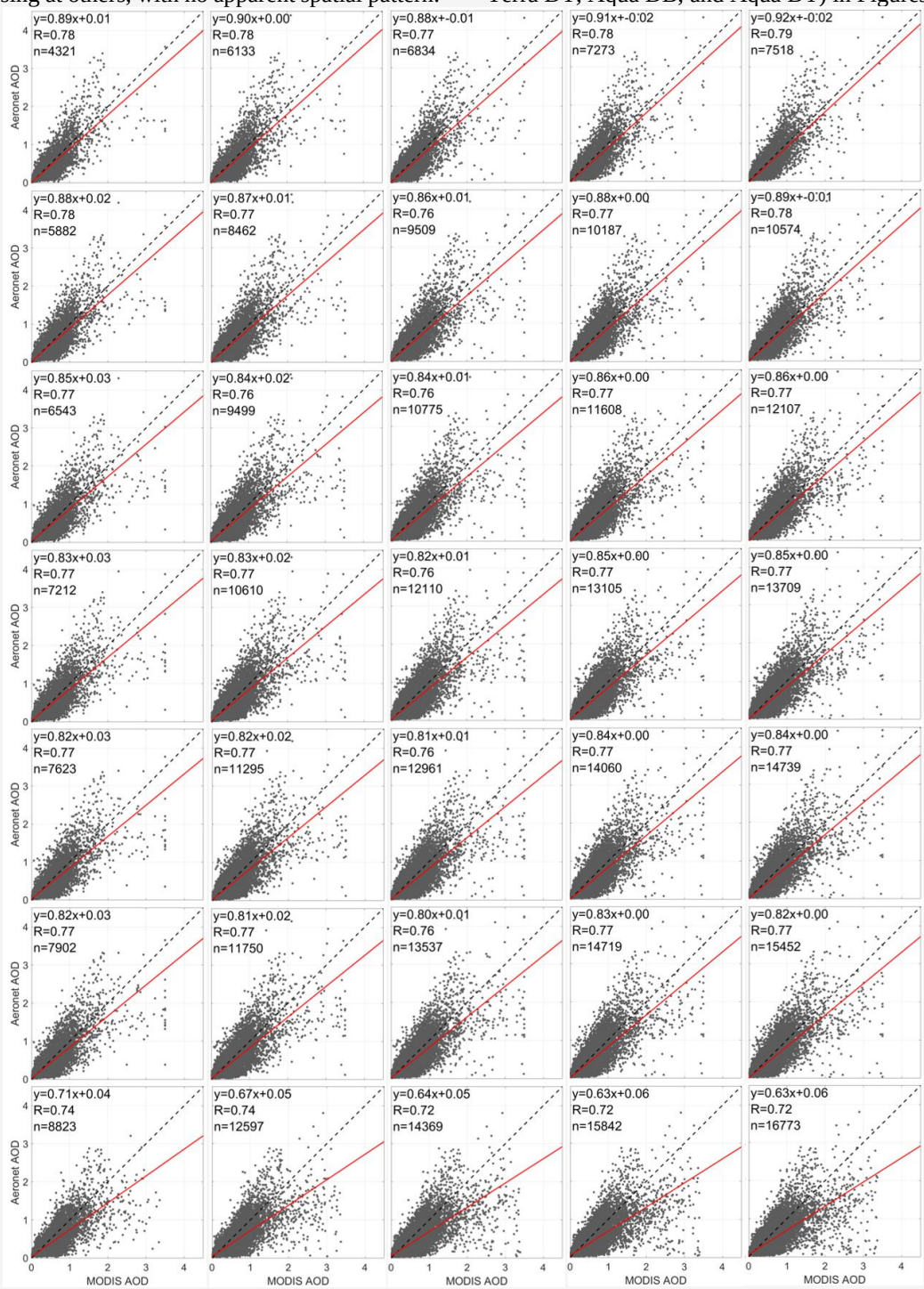

Figure 4: Correlations between Aeronet AOD and MODIS Terra AOD retrieved from the DB algorithm. The slope derived from linear regression (red line), Pearson correlations, and the number of samples are also displayed in each scenario.

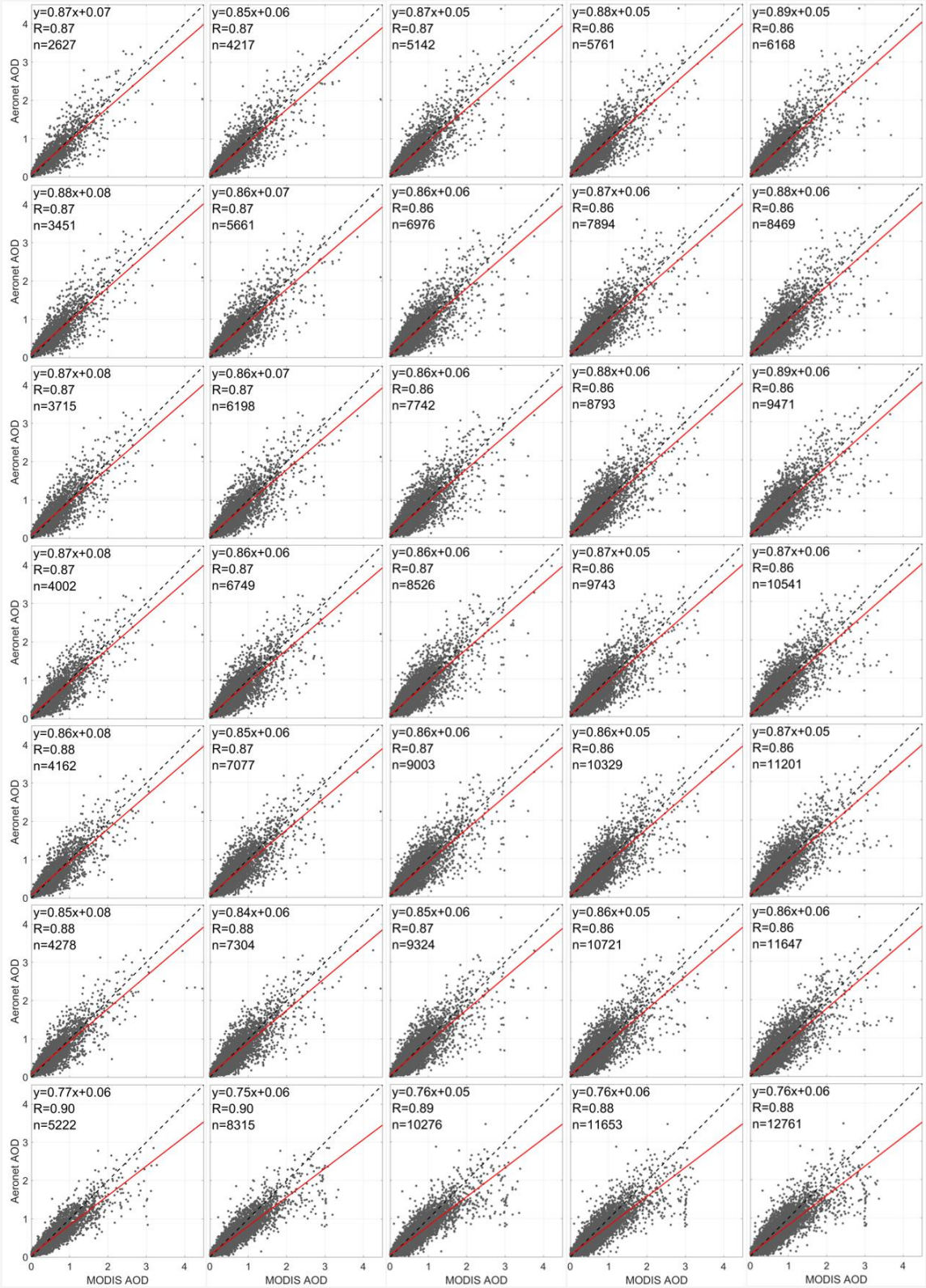

Figure 5: Correlations between AERONET AOD and MODIS Terra AOD retrieved from the DT algorithm. The slope derived from linear regression (red line), Pearson correlations, and the number of samples are also displayed in each scenario.

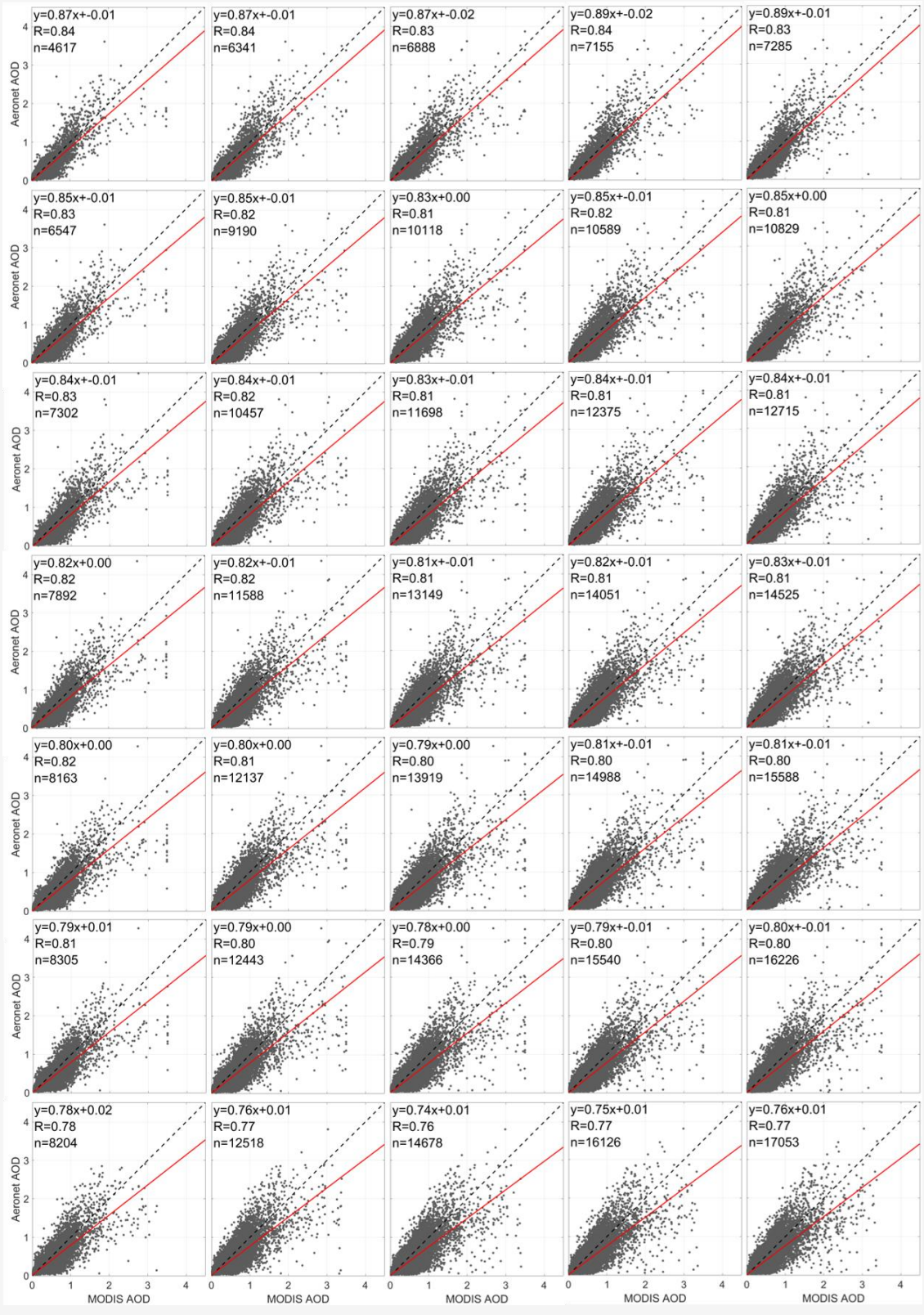

Figure 6: Correlations between AERONET AOD and MODIS Aqua AOD retrieved from the DB algorithm. The slope derived from linear regression (red line), Pearson correlations, and the number of samples are also displayed in each scenario.

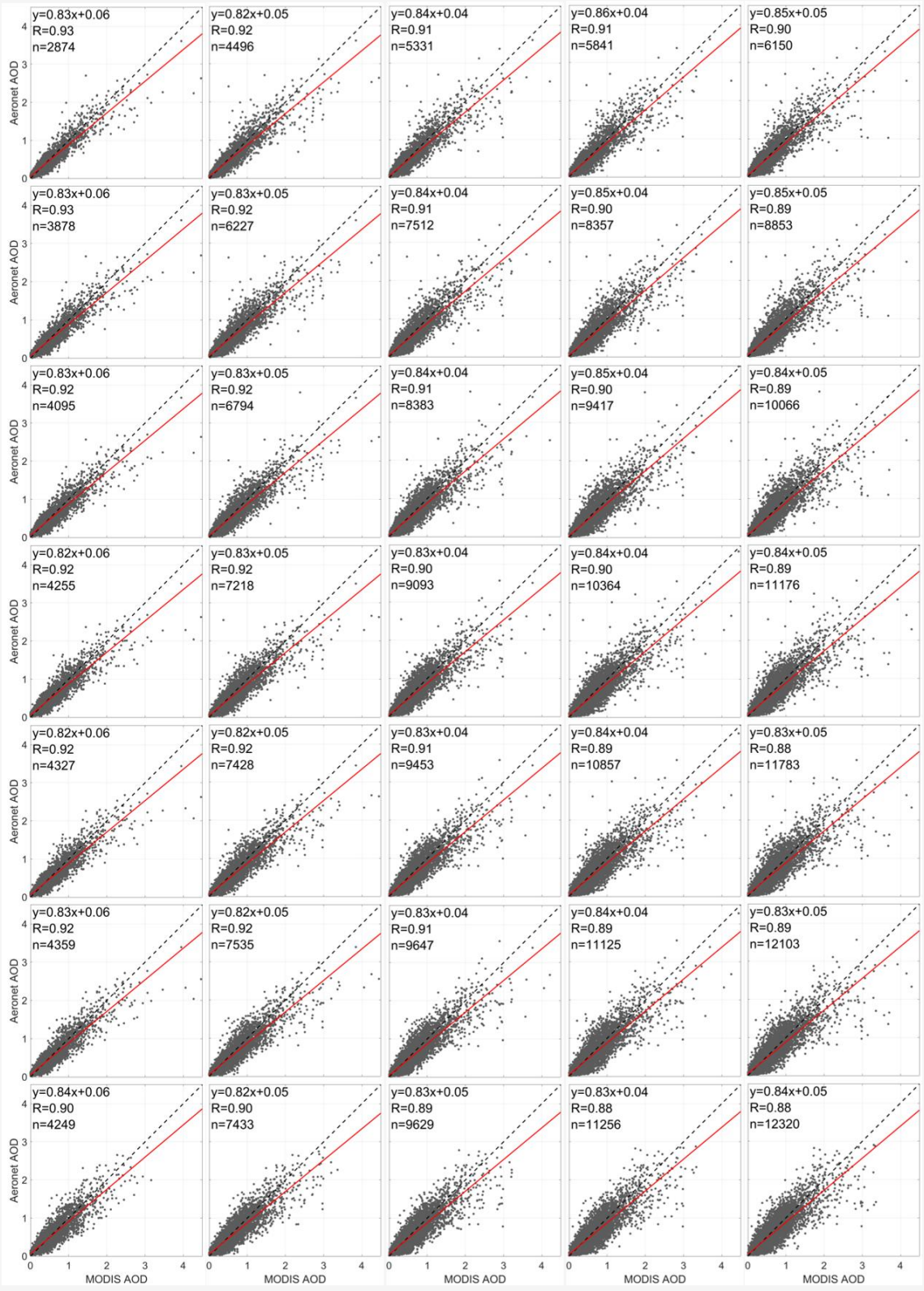

Figure 7: Correlations between AERONET AOD and MODIS Aqua AOD retrieved from the DT algorithm. The slope derived from linear regression (red line), Pearson correlations, and the number of samples are also displayed in each scenario.

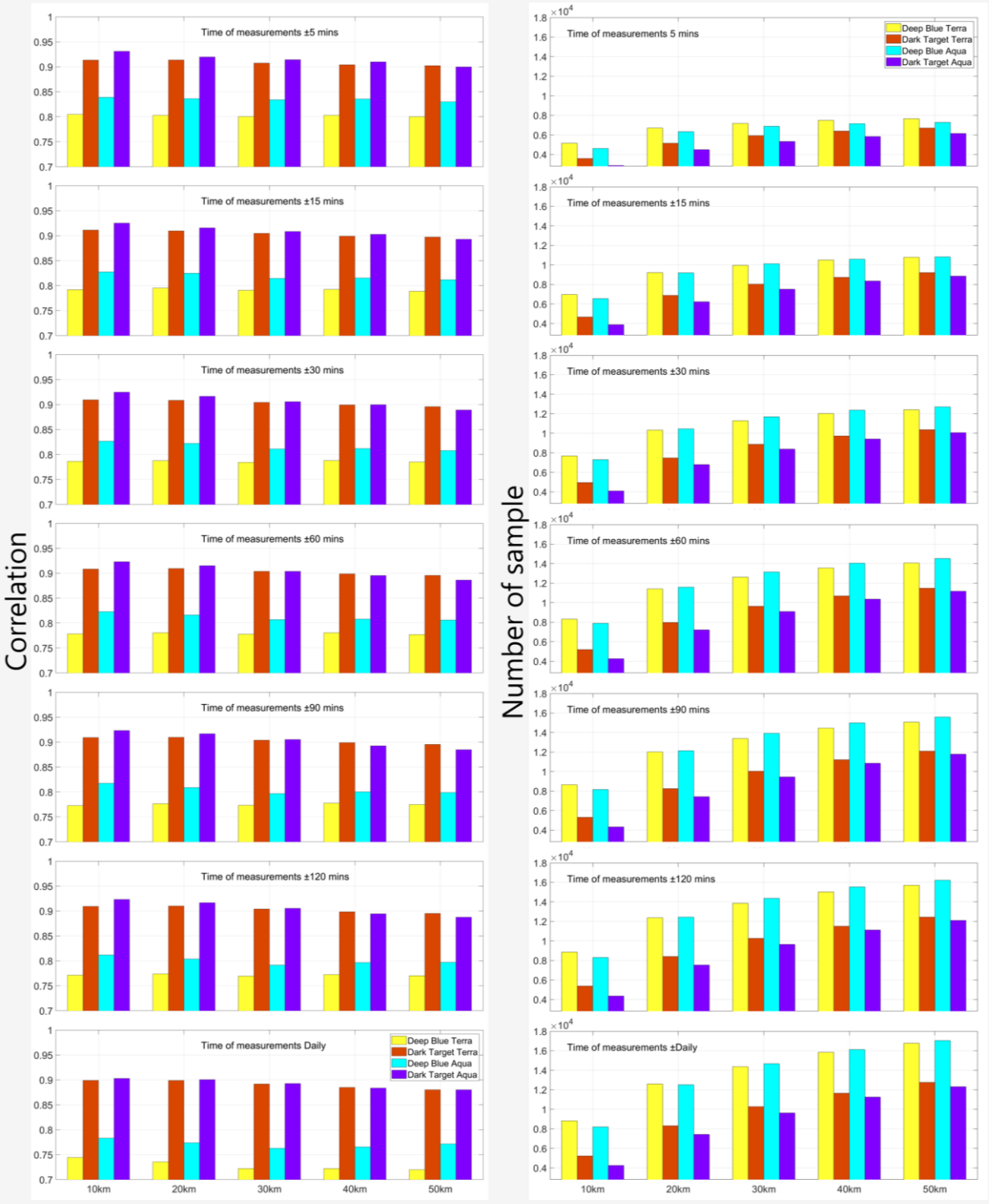

Figure 8: Conclusion of correlations for all scenarios (left). The correlations between AERONET and MODIS Terra DB, Terra DT, Aqua DB, and Aqua DT AOD are shown as yellow, red, cyan, and blue bar charts. They are plotted against different spatial window sizes employed to selected MODIS pixels. Different rows correspond to the time intervals used in select AERONET observations recorded during the specified time period. Conclusion of the number of samples in the correlation calculations (right).

Different subpanel columns correspond to a range of spatial window sizes that include MODIS pixels from AERONET site locations to be averaged. Columns 1-5 are arranged in order of window size (10, 20, 30, 40, and 50 km). Different subpanel rows depict a variation of temporal window periods employed to select AERONET measurements taken during the specified timeframe. Rows 1-6 are organised according to time intervals (±5, ±15, ±30, ±60, ±90 and ±120 minutes) relative to satellite acquisition times, specifically 10:30 a.m. for Terra and 1:30 p.m. for Aqua. Row 7 corresponds to daily data. Each plot displays a slope derived from linear regression, a pairwise linear correlation coefficient (Pearson's correlation) (R), and the number of samples utilised in the comparisons.

We use bar charts to summarise all of the correlation coefficients from each scenario in Figure 8. The results reveal strong correlations between AERONET all of the MODIS products tested. The correlations range from 0.72 to 0.93. In every scenario, MODIS AOD retrieved from the DT algorithm have significantly higher correlations with AERONET AOD than those retrieved from the DB algorithm. The differences between the two products (DB and DT) obtained from Terra and Aqua are 0.10-0.17 and 0.07-0.13, respectively. The differences tend to be larger as the temporal window size extends. The correlations of AOD obtained from the DB (DB) algorithm indicate that the Aqua DB (cyan) has higher correlation than the Terra DB (yellow) in every scenario, with values ranging from 0.02-0.05. On the other hand, the correlations of AOD obtained from the DT algorithm are comparable between the two satellites and the AERONET. The Aqua correlations are slightly higher when we employ spatial window sizes of less than 20 kilometres. The two satellite correlations are nearly equal when we use a spatial window size of 30 kilometres, and the Terra correlations appear to be slightly higher when the window size exceeds 30 kilometres. This could be due to variations in AOD conditions between acquisition times. For the spatiotemporal variations, the correlations appear to be related to temporal window sizes. Specifically, smaller the temporal window size, the better the correlations, particularly the AOD retrieved from the DB algorithm. The decreases are small with AOD retrieved from the DT algorithm.

The variability of spatial window sizes is less significant than that of temporal window sizes. The scenarios between 10 and 20 kilometres are nearly equal, but correlations tend to decrease slightly as window size increases. This variation in spatial perspective is a comparison between point- and area-based observations. Point-based AERONET measurements provide AOD levels at specific locations, whereas area-based observations based on MODIS measurements provide averaged AOD within corresponding areas. However, this study reveals strong correlations between point- and area-based measurements. Thus, the point-based AERONET and area-based MODIS observations are comparable. In this study, correlations are less influenced by spatial window sizes than by temporal window sizes; this weak variation likely corresponds with [26], which propose that AOD levels vary according to the spatial variability of land use and cover. Specifically, even with an enlarged spatial window size, if land use and land cover remain in the same category, the AOD levels from area-based measurements remain comparable to those from point-based measurements.

Furthermore, we employ bar charts to illustrate how the number of samples varies by scenario. For the spatiotemporal variations, the number of samples increases as the spatial and temporal window sizes grow larger. This allows for a higher probability for pairing available observations from both MODIS and AERONET measurements. However, the number of samples of AOD retrieved from DB algorithm is clearly higher than that of the DT algorithm in all scenarios because the DB algorithm has an ability to retrieve more reliable pixels. In terms of DB pixel availability, Terra and Aqua have comparable sample counts. Except for scenarios with a 10-minute window size, the number of Aqua observation samples is slightly higher. Conversely, Terra's DT algorithm provides a higher sample number than Aqua in all scenarios.

In addition, we illustrate the spatial variability of correlations by evaluating temporal correlations at each station, as shown in Figure 9. We find similar information extracted from the overall analysis. The correlations from the DT algorithm (0.8-1.0) appear to be higher than those from the DB algorithm (0.7-1.0) in general. However, the results show that Terra DT appears to have a better correlation than Aqua DT when the correlation analysis is performed separately. The results illustrate lower correlations of observations obtained from the Songkhla Met Sta site in southern Thailand; however, the correlations are still absolutely strong at ~0.8. Furthermore, as presented in [9], the study presents latitudinal variations in the western United States which are assumed to be the result of a variation in MODIS uncertainty; however, we do not find spatial variation in correlations at the latitude and longitude of this study.

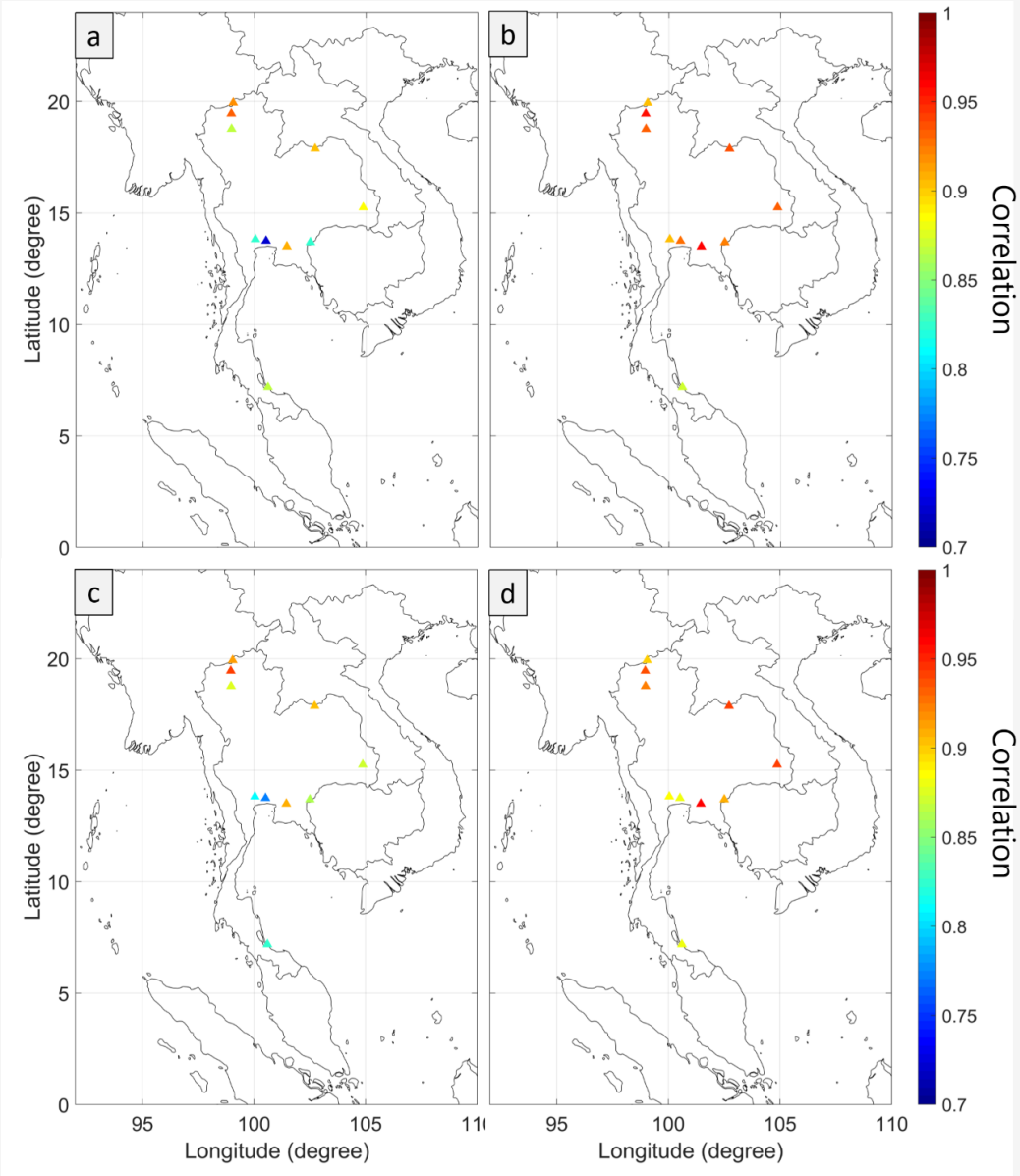

Figure 9: Spatial variability of correlations. The temporal correlations at each station are calculated independently and shown on map: (a) and (b) show correlations between AERONET stations and Terra DB AOD and Terra DT AOD, respectively. (c) and (d) show correlations between AERONET stations and Aqua DB AOD and Aqua DT AOD, respectively.

4. Availabilities of Reliable L2 MODIS Measurements

Thailand is a tropical country, with plenty of rain and cloudy skies throughout the year. Clouds can limit satellite-based observations to retrieve AOD information. We present the spatial variability of the availability of reliable MODIS observations, based on the L2 product, averaged over the last 20 years (2004-2023) of data for each month (Figures 10 and 11). This finding can display the probability of retrieving MODIS observations in order to provide information for managing MODIS data with other observations. As the MODIS pixels are non-uniformly misaligned with regular latitude and longitude alignments, we sampled L2 MODIS data into a regular grid of 0.1˚x0.1˚ (~10x10 km^2). Then, we calculate the ratio of the number of days on which MODIS observations are obtainable to period days (~30 days x 20 years, approximately 600 days).

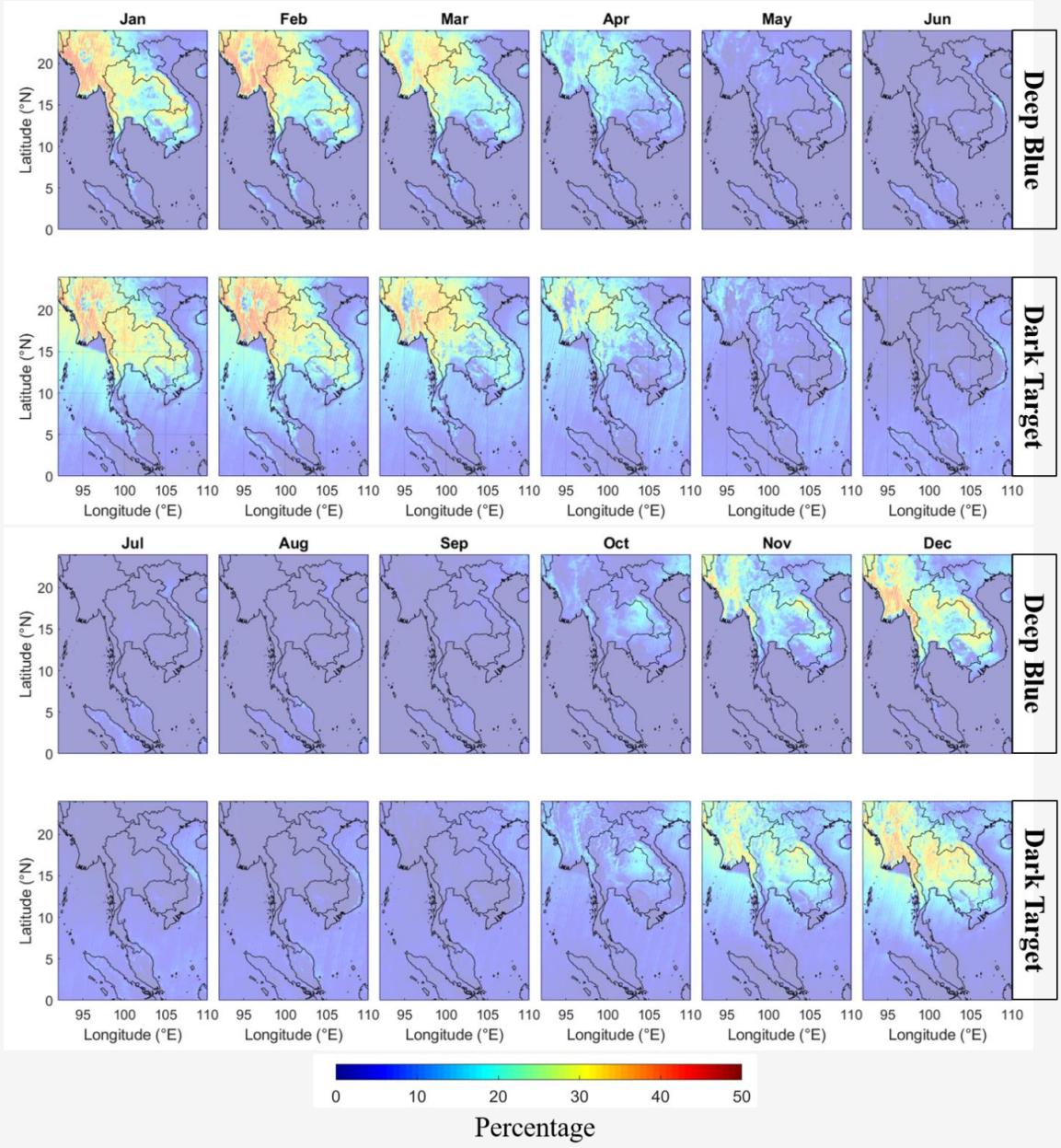

Figure 10: Spatiotemporal variations in the average available rates of Terra observations. The rates are calculated as the ratio of the number of days available for reliable MODIS measurements to the total number of days in the period.

The results indicate that all locations in Thailand and surrounding areas have a probability of reliable MODIS observations of less than 50% for the entire year. From May to October, the chances of MODIS retrieval are low, ranging from 0 to 20% across the entire area. This lack of reliable observations coincides with Thailand's rainy season, which is particularly cloudy. The available rates are higher (20%-50%) during November to April in the northern part of the region, which extends from latitude 13˚ to the north. The highest probabilities occur between December and February. However, the results show that the number of reliable pixels from Terra, which acquires data in the late morning at 10:30 a.m., is consistently higher than Aqua's, which passes by the location in the afternoon at 1:30 p.m., particularly in April, November and December. In addition, the results show that the probabilities of retrieving reliable AOD using DB and DT algorithms are comparable.

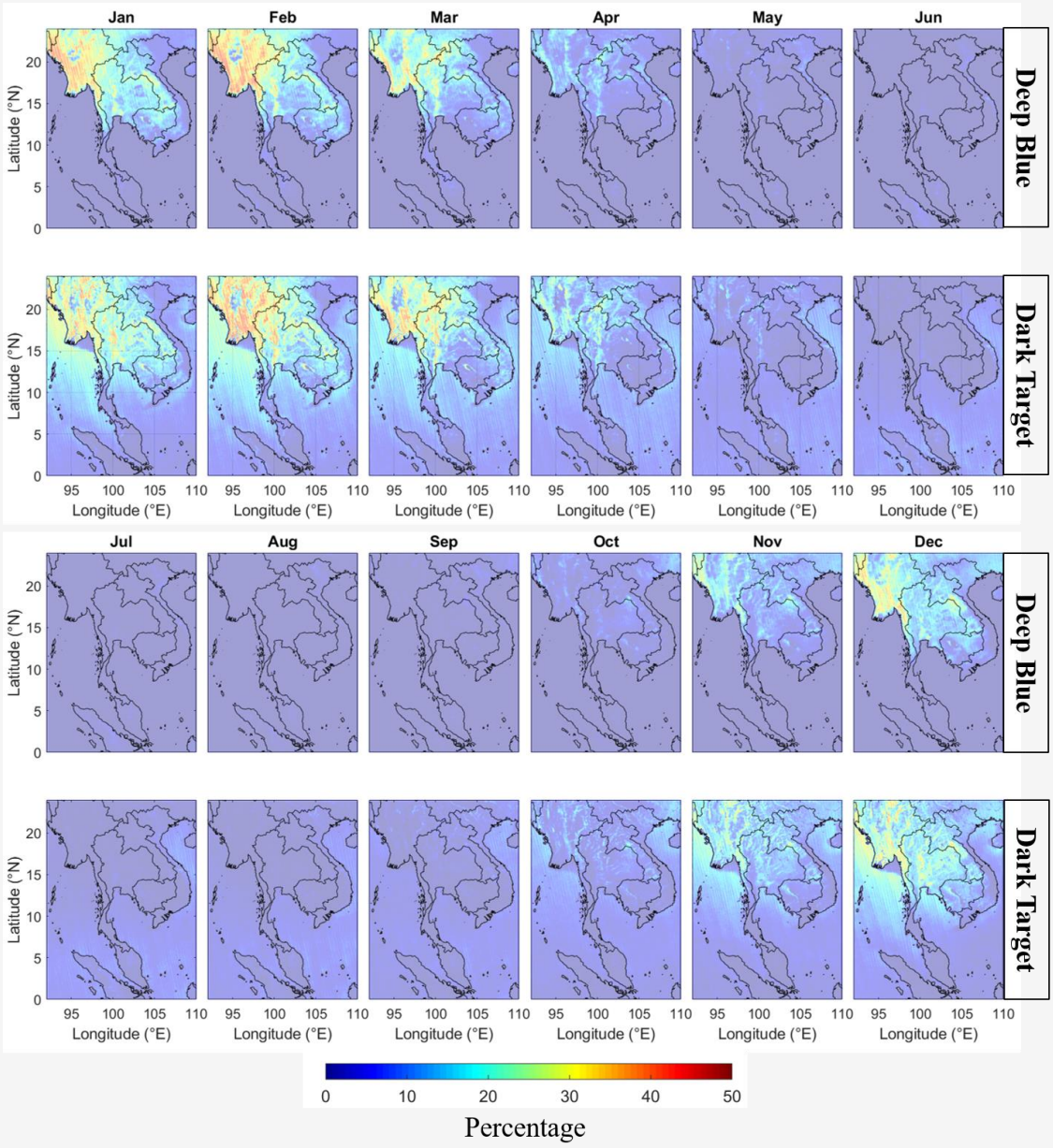

Figure 11: Spatiotemporal variations in the average available rates of Aqua observations. The rates are calculated as the ratio of the number of days available for reliable MODIS measurements to the total number of days in the period.

This demonstrates that the ability to study or analyse AODs from sun-synchronous satellite measurements for Thailand, a tropical region, is dependent on external factors, environmental factors that users cannot control, such as time of day, time of year, and location, rather than internal factors like AOD retrieval algorithms. This indicated that studies may lack comprehensive full-year data and data from specific regions, such as southern Thailand. If we want to take advantage of satellite remote sensing with high spatial coverage, utilising data from geostationary satellites like Himawari, which offers data every 15 minutes, may be a better option. Consequently, the opportunity to obtain data without cloud cover is increased. Furthermore, for monitoring aspects, to compensate for the absence of satellites, more ground-based stations or collaboration with local ground-based data sources, such as Thailand's Pollution Control Department, are required. However, accuracy assessments, availability, and a suitable method of compensation remain necessary.

5. Spatiotemporal AOD over Thailand Observed from MODIS

This chapter presents spatiotemporal characteristics of AOD over Thailand using MODIS datasets collected over a 20-year period from 2004 to 2023. Following the previous chapter, MODIS observations that are not aligned with a regular grid are sampled to a 10-kilometer regular latitude and longitude grid to allow for temporal averaging. Then, we compute monthly averaged AOD for each grid and display them in Figures 12 and 13. Averaging 20 years of data can provide more reliable results due to the increased number of samples used in the averaging. We then use median filtering with a 30-kilometer window size to reduce noise.

Primarily, the results show that high levels of AOD have spread across northern Thailand. The event appears to begin in January and become severe between March and April. Our investigation has revealed that the incident is probably caused by recurring wildfires. The wildfires are most likely caused by agricultural burning, also known as slash and burn agriculture, which is employed at the same time every year. To illustrate this point, we use the Collection 6.1 MODIS Burned Area product [27] to display correlations between high polluted areas defined by AOD levels and locations where burnings are recorded.

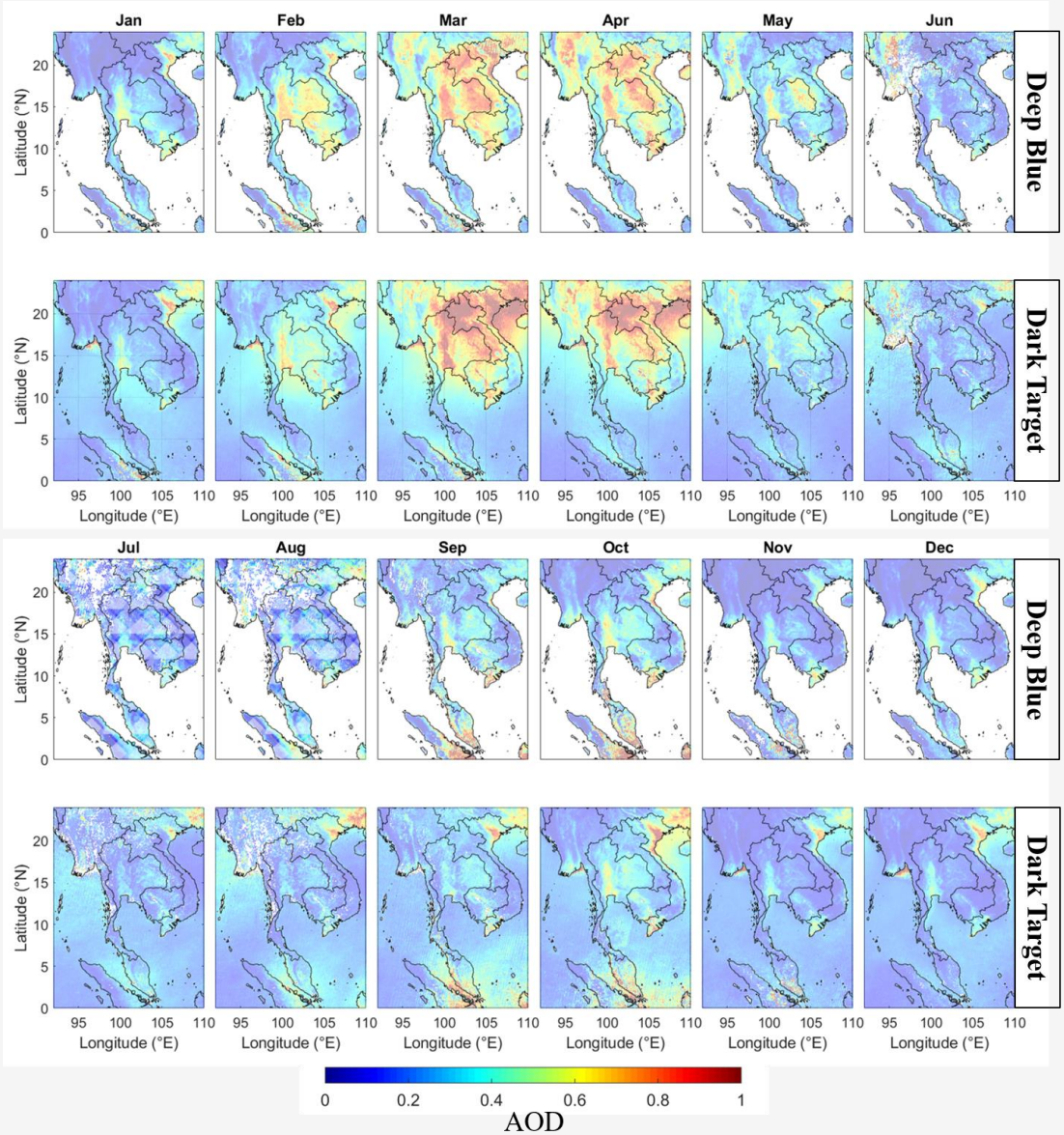

Figure 12: Spatiotemporal variations in the AOD obtained from Terra observations.

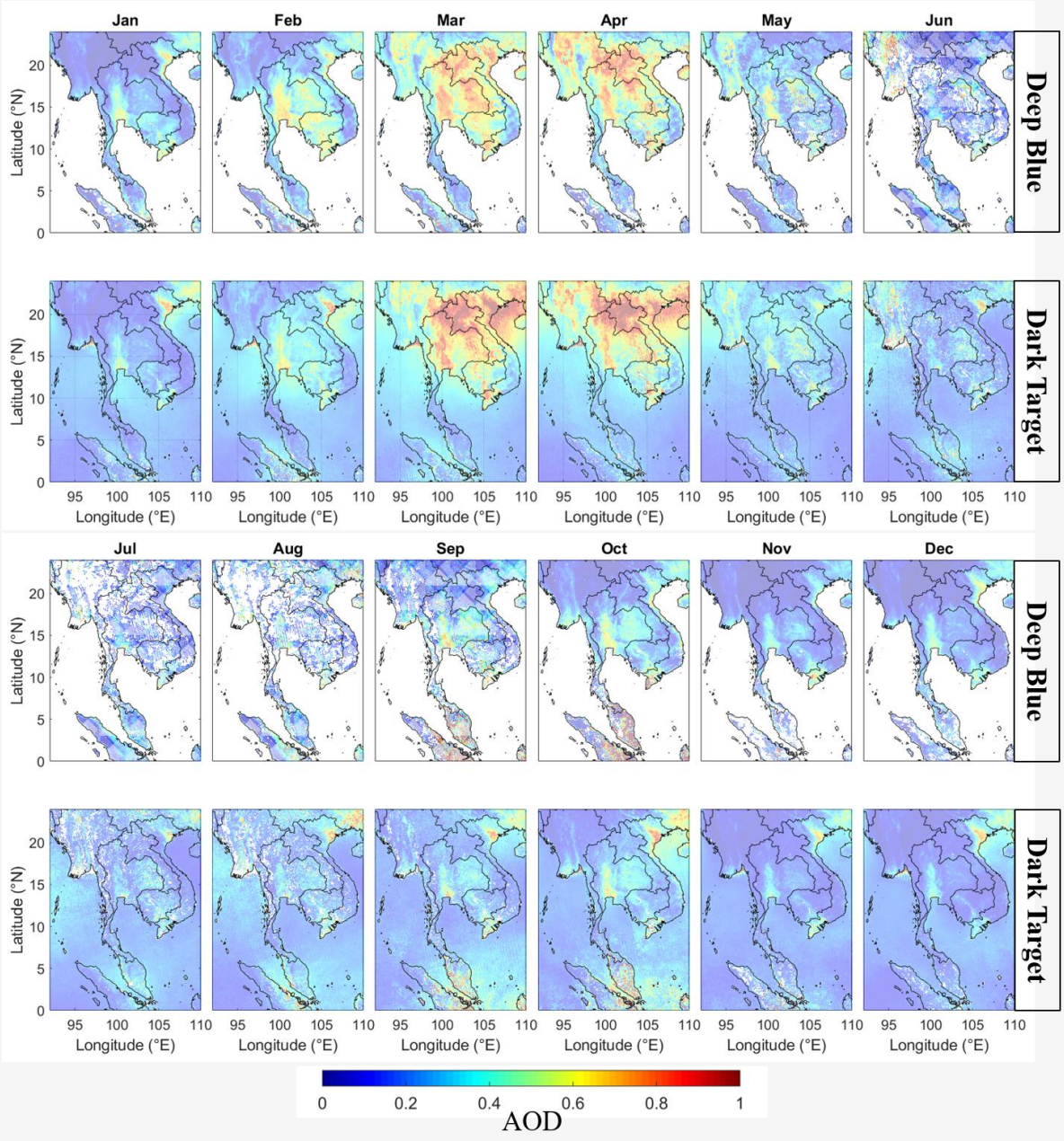

Figure 13: Spatiotemporal variations in the AOD obtained from Aqua observations.

A forest fire substantially modifies the characteristics of the ground surface in the impacted region, such as the accumulation of charcoal and ash or changes of vegetative properties. The product strategy is to identify sudden variations in surface reflectance and define fire locations with time of occurrence using a 500-meter resolution grid. In this study, we specifically use GeoTiff MCD64 monthly Burn Date, which was developed by the University of Maryland. The data shows that wildfires in the region occur annually between January and April. We depict hotspots of MODIS burned areas that occurred in 2010 and 2014 in Figure 14. as an example. We can see that the spatial extents of areas with high MODIS AOD correspond fairly well to the shape of the hotspot distributions. In January, hotspots in Thailand start to occurring but they are still sparse. However, we find burned areas are concentrated along the Thai-Cambodian border. The AODs from the DB algorithm appear to correspond to this occurring event, but we cannot see a clear indication in AODs from the DT algorithm, from both Terra and Aqua observations.

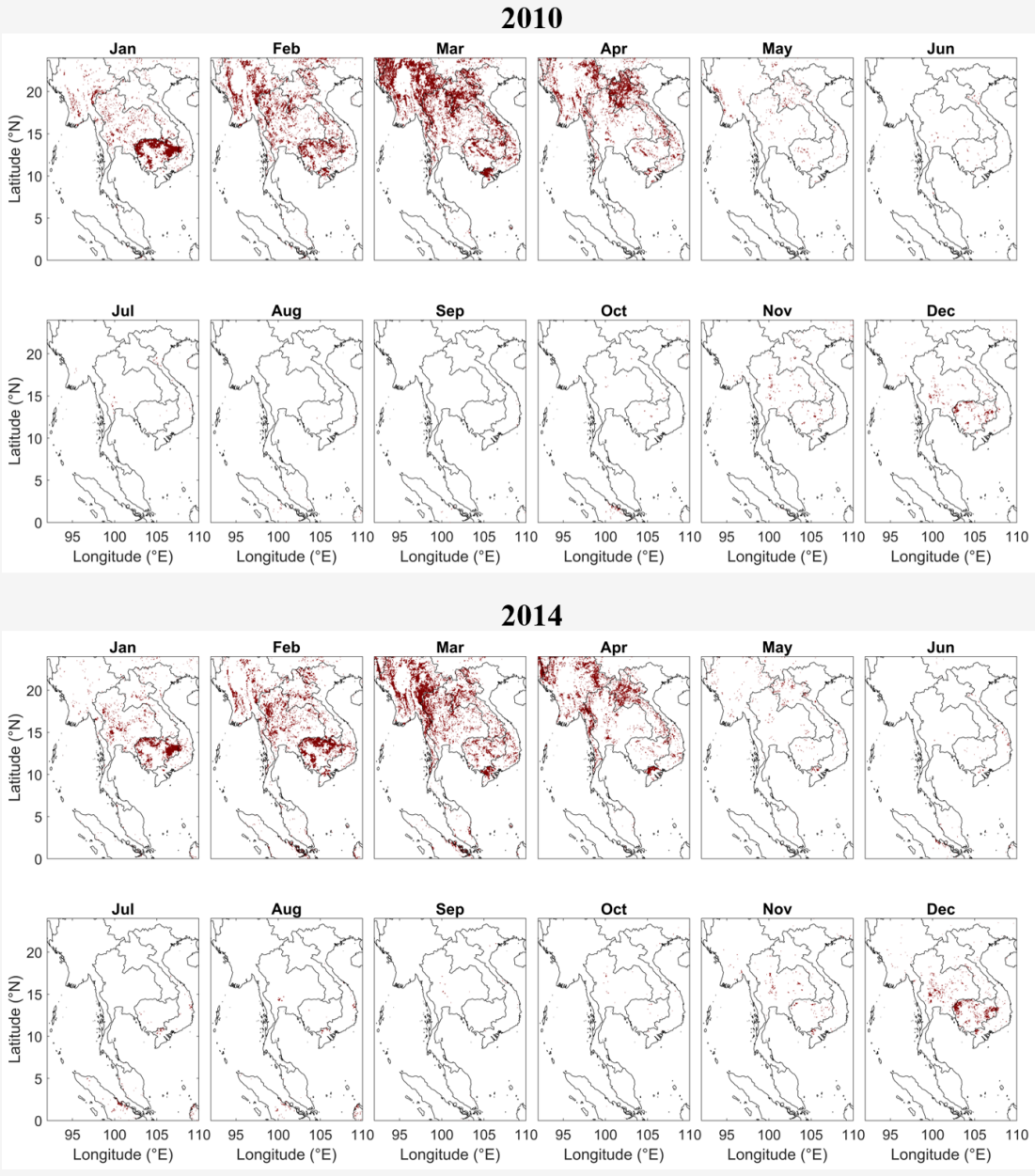

Figure 14: Spatial distribution of hotspots based on the MODIS burned area product. The data show the predicted locations of fires in Thailand and the surrounding countries in 2010 and 2014.

In February, the burned areas spread widely, as does the distribution of areas with higher AOD levels, particularly in eastern Thailand. In March and April, hotspots are densely concentrated in extensive areas surrounding the borders of northern Thailand, Laos, and Myanmar. All MODIS products exhibit significantly high levels of AOD in the relevant areas.

Another polluted area of the region occurs during September and October. During this period, high AOD levels are recorded in southern Thailand, Malaysia, Singapore, and Indonesia. The MODIS burned area product does not reveal a significant number of burned activities in the specific areas. However, the pollution during this period coincides with a season of agricultural burn in many parts of Indonesia. We show an example of a MODIS burned area over Indonesia during the specified time period in Figure 15. The burning aerosols can be transported by winds and spread across the region, including southern Thailand.

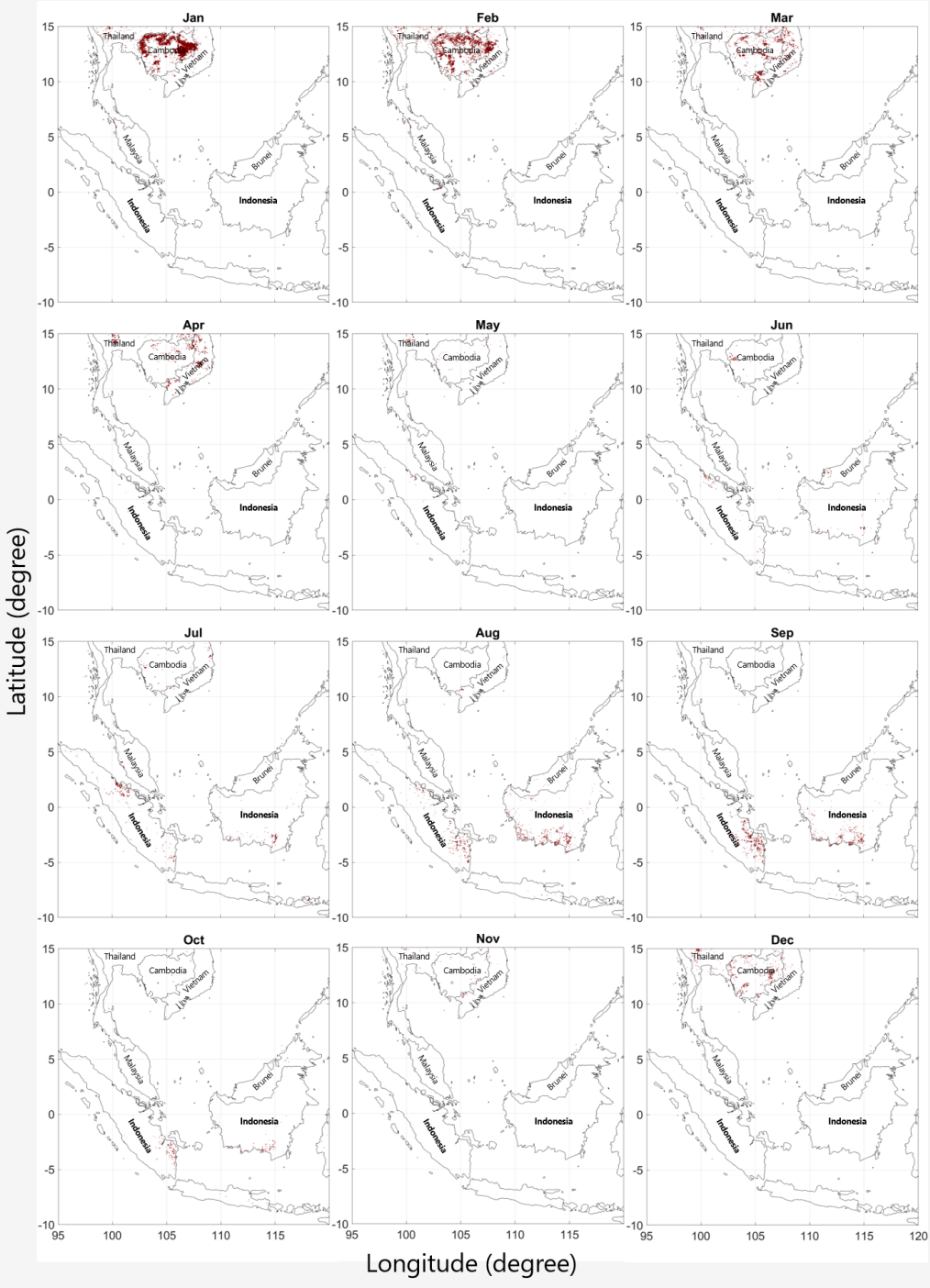

Figure 15: Spatial distribution of hotspots based on the MODIS burned area product. The data show the predicted locations of fires in Indonesia in 2011.

As shown in the results, the AOD products from the DT algorithm can provide a better illustration for this investigation because the technique can estimate AOD in ocean area. The distribution of high AOD levels across Malaysia begins in July-August and expands with higher levels of AOD in September and October.

Apart from the two events, MODIS observations do not show significantly high levels over widespread areas. The areas with high AOD levels appear to be related to local activities. The results display that pollution in greater

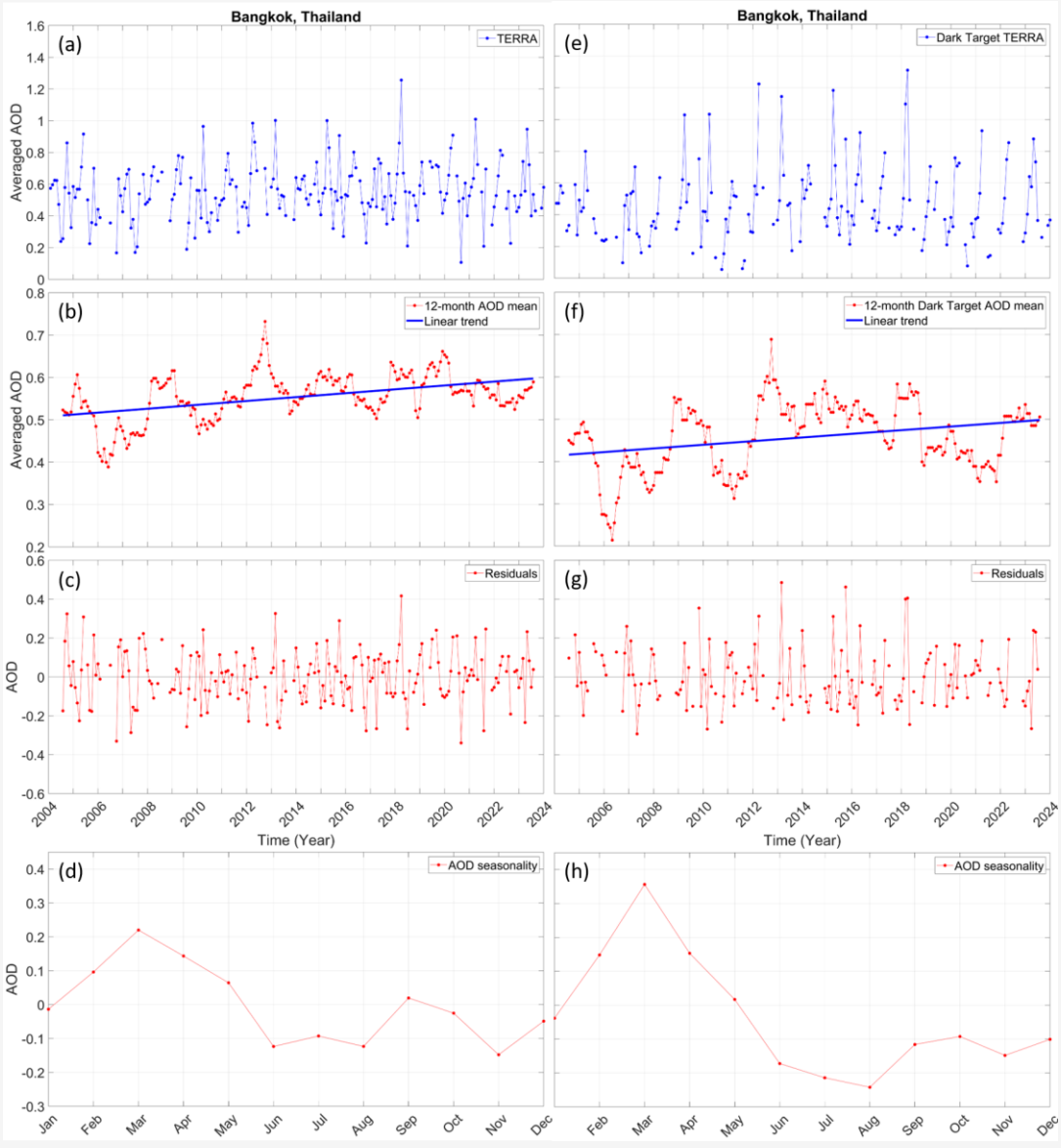

Figure 16: Time-series compositions of AOD over Bangkok: (a) Monthly average AOD time series from the DB algorithm (b) Estimate Annual mean AOD levels (T) with linear models that best fit the data. (c) Residuals between the original observations and the combination of trend (T) and seasonality (S) displayed in (d), (e), (f), (g) and (h) show the same parameters, but from the DT algorithm.

Bangkok is high throughout the year, including during the rainy season. This is likely attributable to significant traffic congestion in the city. Our results also indicate high AOD levels year-round in Ha Noi area of Vietnam, an industrial zone that has experienced rapid growth in recent years.

In this study of pollution in Thailand, we take advantage of MODIS, which has a long-term record of AOD levels with high spatial coverage and resolution, to investigate temporal characteristics of AOD levels in two cities: Bangkok, Thailand's capital city, which experiences air pollution all year, and Chiang Mai, Thailand's second largest city, which faces air pollution from wildfires in the summer and has been ranked as the top most polluted city many times. First, due to the frequent absence of reliable measurements over Thailand, a tropical region, we estimate monthly AOD using a 10-kilometer regular grid and then perform median filtering with a 30x30 km window size to reduce noise. We select the averaged AOD over Bangkok and Chiang Mai to present as time-series data in Figures 16 and 17.

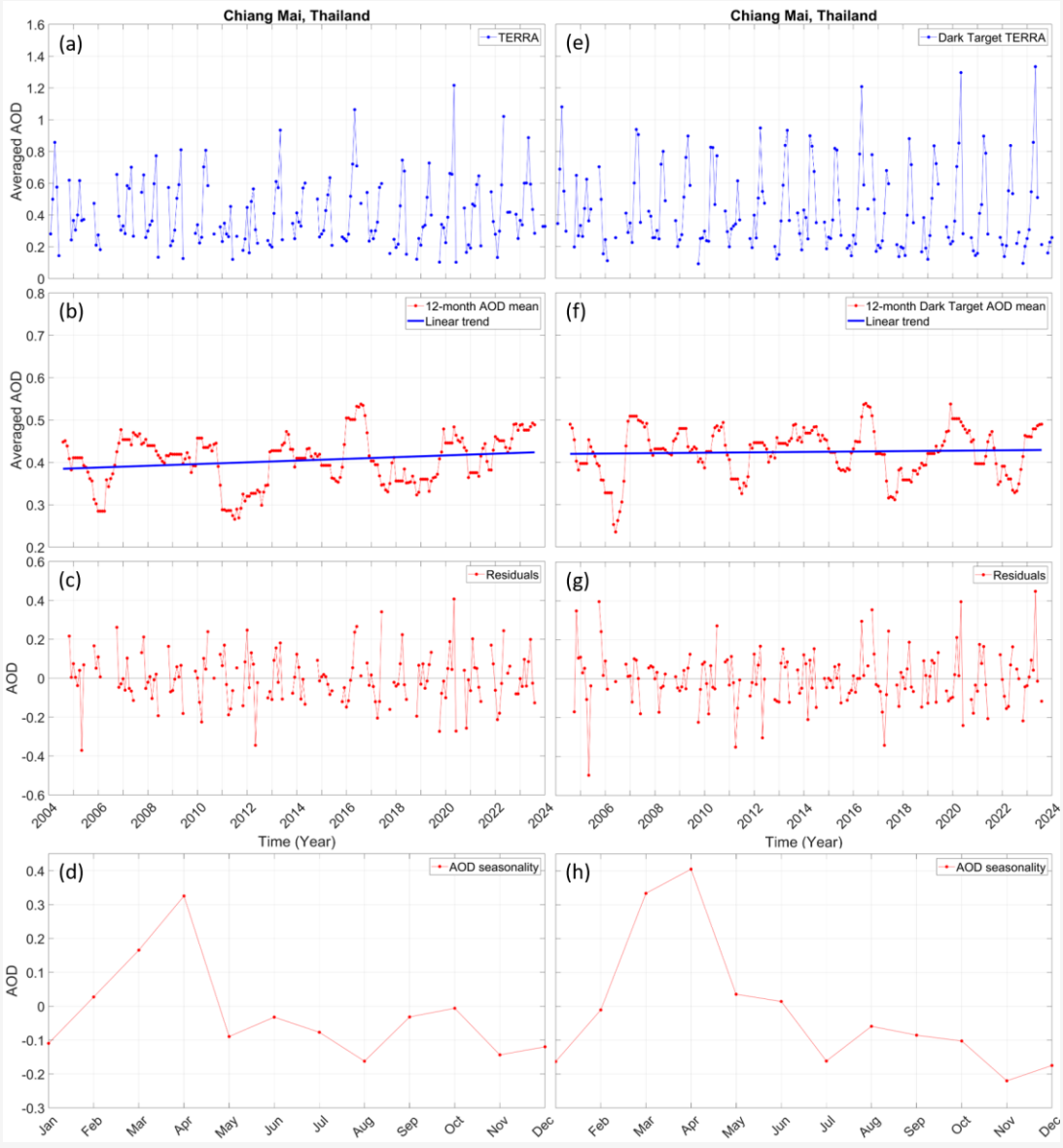

Figure 17: Time-series compositions of AOD over Chiang Mai: (a) Monthly average AOD time series from the DB algorithm (b) Estimate Annual mean AOD levels (T) with linear models that best fit the data. (c) Residuals between the original observations and the combination of trend (T) and seasonality (S) displayed in (d), (e), (f), (g), and (h) show the same parameters, but from the DT algorithm.

The time series is then decomposed into three components: trend (T), seasonality (S), and noise (N). We first extracted annual mean AOD levels (T) using a moving average with a one-year window to avoid seasonality. The original time series is then detrended using the estimated trends, and the averaged AOD at each month is calculated using 20 years of data to retrieve seasonality (S). We also present noise (N), which is a residual between the original data and the combination of the estimated trend and seasonality. The noise can be used to study occasional events because it can be investigated to identify anomalous AOD levels. However, it is outside the scope of this study.

According to the results, we find that long-term trends in AOD levels in Bangkok and have increased even with high fluctuation. We perform a linear regression with the estimated long-term trends and present the results as blue lines. The long-term average AODs over Bangkok increased by about 0.1 over the last 20 years and are about 0.55 and 0.60 on average, in 2023 from DB and DT, respectively, as identified by the end point of the estimated linear trend, blue lines.

The estimated seasonality of Bangkok AOD shows high annual variations, about 0.3 and 0.6, from DB and DT, respectively, and appears to peak during February-April. According to the Chiang Mai time series, we find high pollution during the summer every year. This means that the northern Thailand region has been experienced recurring wildfire pollution for the past two decades. Both the DB and DT algorithms indicate that long-term trends of AOD in Chaing Mai are stable and average around 0.40 which are lower than Bangkok. The seasonality (S) exhibits an average annual variation of approximately 0.55-0.60, with a peak in March and April due to the aforementioned wildfires.

6. Conclusions

This study analyses overview of long-term records of MODIS observations over Thailand with measurements from 10 AERONET sites located across Thailand. Firstly, to illustrate overview AOD characteristics, this study examines the AERONET ground-surface AOD measurements which is more robust to surface AOD that affect human health. We find significant high levels of AOD from stations located in northern Thailand in every summer. Furthermore, due to its high temporal resolution, we can display an hourly average variation in daytime. The results present that the daytime variations are only significance in summer and their patterns vary by stations. A majority pattern of the AOD levels in summer is increase in early morning (6 a.m. - 8 a.m.) and decrease throughout the rest of the day. This study examines overall correlations between the AERONET measurements and several MODIS products (i.e. Terra DB, Terra DT, Aqua DB, Aqua DT) with variance of spatiotemporal window sizes. Primarily, all of the product in all comparison scenarios show strong correlations (0.72-0.93) between the satellite and ground measurements in Thailand. In general, the AOD retrieved from DT algorithm represent significantly higher correlations than from the DB algorithm, from 0.07 to 0.17. This can be due to that Thailand has lot of vegetated areas, which suit with DT method, and has low number of bright surfaces, such as arid, which is an area type that correspond to the advantage of DB technique. This study also find that correlations exploited from Aqua's observations are higher than Terra's. The investigation of spatiotemporal variations of window sizes represent that the correlations are sensitive to ranges of time periods than spatial distances from the AERONET sites to select MODIS pixels to be averaged. Furthermore, as Thailand is in tropical zone which is covered by clouds, limiting satellite measurements, throughout the year, this study also displays monthly spatial variations of available rates that we can expect reliable measurements. This study also examines spatiotemporal characteristics of AOD using the MODIS observations.

The results show significant high levels of AOD widespread across northern Thailand and also in Laos and Myanmar during summer. Our investigations from MODIS burned area product identify that the severe pollutions are probably caused from wildfires as the location of high polluted areas correlate with location of hotspot occurrences. Furthermore, the time series analysis presents that northern Thailand has experienced the events in every summer for 20 years. Furthermore, the maps of averaged AOD detect high level of AOD in southern Thailand, Malaysia, Singapore, and Indonesia during September and October. As there are no significant hotspots reported from the MODIS burned area product in the region; however, the event coincides with the period of employing agricultural burning in Indonesia. The aerosols can be carried by winds into the region. We also decompose the time series of AOD over Bangkok and Chiang Mai, two major cities in Thailand. The long-term trends over both cities show increasing of AOD. All of these results can be useful information for using the observations including secondary process such as filtering, before injecting them into simulations or Machine Learning algorithms in the future. This can also guide what we can get from the MODIS observations and gaps we need to fill in to get optimize monitoring air pollution for Thailand.

Apart from the technical findings of this study, we conclude that Thailand has experienced significant air pollution from two sources: wildfires in northern Thailand and traffic congestion in Bangkok. Significant numbers of wildfires in the north are attributed to human activity. Thailand enforces stringent legislation prohibiting forest burning; however, its implementation is restricted only to national parks. Consequently, this legislation does not regulate alternative forms of burning, such as slash-and-burn agriculture. Usually, when getting into summer that always experience high air pollution, an announcement will be made requesting cooperation in refraining from any type of open burning. However, this study shows that these methods are still ineffective, as recurring highly severe air pollution in northern Thailand has been detected every year for the past 20 years with no decreasing trend. This can indicate that additional measures are required to mitigate the pollution.

For the latter sources, Bangkok's air pollution is caused by high traffic congestion, excessive vehicle combustion, and long periods of time spent on the road. Despite Thailand's law prohibiting vehicles with ineffective combustion and generating pollution above standard, as well as the long-term policy of continuously establishing infrastructures to cover travel throughout Bangkok over the last two decades, air pollution in Bangkok remains severe, with an increasing trend, as presented in this study. However, apart from the government efforts, global trends of transitioning from biomass-burning vehicles to electric vehicles can play a significant role in reducing pollution in urban areas, applicable not only to Bangkok but to cities around the globe.

References

[1] State of Global Air Report, (2024). *World Health Organization (WHO)*. [Online]. Available: https://www.stateofglobalair.org/resources/report/state-global-air-report-2024. [Accessed Sep. 09, 2024].

[2] Table of Gross Regional and Provincial Product, (2022). *Office of the National Economic and Social Development Council, Thailand*. [Online]. Available: https://www.nesdc.go.th/nesdb_en/more_news.php?cid=156&filename=index. [Accessed Sep. 24, 2024].

[3] Tourism Statistics, (2023), Classify by Region and Province, 2023. *Ministry of Tourism & Sports (Thailand)*. [Online]. Available: https://www.mots.go.th/news/category/704. [Accessed Sep. 15, 2024].

[4] Tian, X., Tang, C., Wu, X., Yang, J., Zhao, F. and Liu, D., (2023). The Global Spatial-Temporal Distribution and EOF Analysis of AOD Based on Modis Data during 2003–2021. *Atmospheric Environment*, Vol. 302. https://doi.org/10.1016/j.atmosenv.2023.119722.

[5] Bibi, H., Alam, K., Chishtie, F., Bibi, S., Shahid, I. and Blaschke, T., (2015). Intercomparison of MODIS, MISR, OMI, and Calipso Aerosol Optical Depth Retrievals for Four Locations on the Indo-Gangetic Plains and Validation against AERONET Data. *Atmospheric Environment*, Vol. 111, 113-126. https://doi.org/10.1016/j.atmosenv.2015.04.013.

[6] Hersey, S. P., Garland, R. M., Crosbie, E., Shingler, T., Sorooshian, A., Piketh, S. and Burger, R., (2015). An Overview of Regional and Local Characteristics of Aerosols in South Africa Using Satellite, Ground, and Modeling Data. *Atmospheric Chemistry and Physics*, Vol. 15(8), 4259-4278. https://doi.org/10.5194/acp-15-4259-2015.

[7] Kim, P. S., Jacob, D. J., Fisher, J. A., Travis, K., Yu, K., Zhu, L., Yantosca, R. M., Sulprizio, M., Jimenez, J. L. and Campuzano-Jost, P., (2015). Sources, Seasonality, and Trends of Southeast Us Aerosol: An Integrated Analysis of Surface, Aircraft, and Satellite Observations with the Geos-Chem Chemical Transport Model. *Atmospheric Chemistry and Physics*, Vol. 15(18), 10411-10433. https://doi.org/10.5194/acp-15-10411-2015.

[8] Drury, E., Jacob, D. J., Spurr, R. J., Wang, J., Shinozuka, Y., Anderson, B. E., Clarke, A. D., Dibb, J., McNaughton, C. and Weber, R., (2010). Synthesis of Satellite (MODIS), Aircraft (ICARTT), and Surface (Improve, EPA - AQS, AERONET) Aerosol Observations over Eastern North America to Improve Modis Aerosol Retrievals and Constrain Surface Aerosol Concentrations and Sources. *Journal of Geophysical Research: Atmospheres*, Vol. 115(D14). https://doi.org/10.1029/2009JD012629.

[9] Eibedingil, I. G., Gill, T. E., Van Pelt, R. S. and Tong, D. Q., (2021). Comparison of Aerosol Optical Depth from Modis Product Collection 6.1 and AERONET in the Western United States. *Remote Sensing*, Vol. 13(12). https://doi.org/10.3390/rs13122316.

[10] Hu, K., Kumar, K. R., Kang, N., Boiyo, R. and Wu, J., (2018). Spatiotemporal Characteristics of Aerosols and their Trends over Mainland China with the Recent Collection 6 MODIS and OMI Satellite Datasets. *Environmental Science and Pollution Research*, Vol. 25, 6909-6927. https://doi.org/10.1007/s11356-017-0715-6.

[11] Zhang, W., Gu, X., Xu, H., Yu, T. and Zheng, F., (2016). Assessment of OMI near-UV Aerosol Optical Depth over Central and East Asia. *Journal of Geophysical Research: Atmospheres*, Vol. 121(1), 382-398. https://doi.org/10.1002/2015JD024103.

[12] Reid, J. S., Hyer, E. J., Johnson, R. S., Holben, B. N., Yokelson, R. J., Zhang, J., Campbell, J. R., Christopher, S. A., Di Girolamo, L. and Giglio, L., (2013). Observing and Understanding the Southeast Asian Aerosol System by Remote Sensing: An Initial Review and Analysis for the Seven Southeast Asian Studies (7seas) Program. *Atmospheric Research*, Vol. 122, 403-468. https://doi.org/10.1016/j.atmosres.2012.06.005

[13] Nguyen, T. T., Pham, H. V., Lasko, K., Bui, M. T., Laffly, D., Jourdan, A. and Bui, H. Q., (2019). Spatiotemporal Analysis of Ground and Satellite-Based Aerosol for Air Quality Assessment in the Southeast Asia Region. *Environmental Pollution*, Vol. 255. https://doi.org/10.1016/j.envpol.2019.113106.

[14] Pilahome, O., Ninssawan, W., Jankondee, Y., Janjai, S. and Kumharn, W., (2022). Long-Term Variations and Comparison of Aerosol Optical Properties Based on Modis and Ground-Based Data in Thailand. *Atmospheric Environment*, Vol. 286. https://doi.org/10.1016/j.atmosenv.2022.119218.

[15] Hsu, N. C., (2017). Changes to Modis Deep Blue Aerosol Products between Collection 6 and Collection 6.1. *NASA GSFC: Greenbelt, MD, USA*. 1-9. [Online]. Available: https://atmosphere-imager.gsfc.nasa.gov/sites/default/files/ModAtmo/modis_deep_blue_c61_changes2.pdf. [Accessed Oct. 05, 2024].

[16] Lalaeng, S., Thanasang, T., Puttinet, P., Srireuan, N., and Chavanavesskul, S. (2024). The Relationship between PM2.5 and Solar Cell Electricity Generation Using Aerosol Optical Depth (AOD). *International Journal of Geoinformatics*, Vol. 21(1), 83–96. https://doi.org/10.52939/ijg.v21i1.3797.

[17] Anderson, T. L., Charlson, R. J., Winker, D. M., Ogren, J. A. and Holmén, K., (2003). Mesoscale Variations of Tropospheric Aerosols. *Journal of the Atmospheric Sciences*, Vol. 60(1), 119-136. https://doi.org/10.1175/1520-0469(2003)060<0119:MVOTA>2.0.CO;2.

[18] Wei, J., Li, Z., Peng, Y. and Sun, L., (2019). Modis Collection 6.1 Aerosol Optical Depth Products over Land and Ocean: Validation and Comparison. *Atmospheric Environment*, Vol. 201, 428-440. https://doi.org/10.1016/j.atmosenv.2018.12.004.

[19] Final report of Forest Area Information Project 2023. *Forest Land Management Office (Thailand) (2024)*. [Online]. Available: https://www.forest.go.th/land/category/paper/. [Accessed Oct. 05, 2024].

[20] Eck, T. F., Holben, B., Reid, J., Dubovik, O., Smirnov, A., O'neill, N., Slutsker, I. and Kinne, S., (1999). Wavelength Dependence of the Optical Depth of Biomass Burning, Urban, and Desert Dust Aerosols. *Journal of Geophysical Research: Atmospheres*, Vol. 104(D24), 31333-31349. https://doi.org/10.1029/1999JD900923.

[21] Holben, B. N., Eck, T. F., Slutsker, I. a., Tanré, D., Buis, J., Setzer, A., Vermote, E., Reagan, J. A., Kaufman, Y. and Nakajima, T., (1998). AERONET a Federated Instrument Network and Data Archive for Aerosol Characterization. *Remote Sensing of Environment*, Vol. 66(1), 1-16. https://doi.org/10.1016/S0034-4257(98)00031-5.

[22] Rainwater, M. and Gregory, L., (2005). *Cimel Sunphotometer (Csphot) Handbook*. Technical Report ARM TR-056, US Department of Energy Atmospheric Radiation Measurement Program.

[23] Shi, Y., Zhang, J., Reid, J., Holben, B., Hyer, E. and Curtis, C., (2011). An Analysis of the Collection 5 Modis over-Ocean Aerosol Optical Depth Product for its Implication in Aerosol Assimilation. *Atmospheric Chemistry and Physics*, Vol. 11(2), 557-565. https://doi.org/10.5194/acp-11-557-2011.

[24] Yang, J. and Hu, M., (2018). Filling the Missing Data Gaps of Daily MODIS AOD Using Spatiotemporal Interpolation. *Science of the Total Environment*, Vol. 633, 677-683. https://doi.org/10.1016/j.scitotenv.2018.03.202

[25] Zhang, Y., Yu, H., Eck, T. F., Smirnov, A., Chin, M., Remer, L. A., Bian, H., Tan, Q., Levy, R. and Holben, B. N., (2012). AEROSOL Daytime Variations Over North and South America Derived from Multiyear AERONET Measurements. *Journal of Geophysical Research: Atmospheres*, Vol. 117(D5). https://doi.org/10.1029/2011JD017242.

[26] Sharma, V., Ghosh, S., Singh, S., Vishwakarma, D. K., Al-Ansari, N., Tiwari, R. K. and Kuriqi, A., (2022). Spatial Variation and Relation of Aerosol Optical Depth with LULC and Spectral Indices. *Atmosphere*, Vol. 13(12). https://doi.org/10.3390/atmos13121992.

[27] Giglio, L., Boschetti, L., Roy, D. P., Humber, M. L. and Justice, C. O., (2018). The Collection 6 MODIS Burned Area Mapping Algorithm and Product. *Remote Sensing of Environment*, Vol. 217, 72-85. https://doi.org/10.1016/j.rse.2018.08.005.